Supporting Information

Melero et al. 10.1073/pnas.1015520107

SI Text

SI Materials and Methods. ***Protein expression and purification.*** Human p53 (1–393) was expressed and purified as described previously (1). Briefly, p53 residues 1–393 were cloned into a pET24a-HLTV plasmid containing a 5′ extension expressing a His_6-tag, a lipoyl domain, and a TEV protease cleavage site. A superstable p53 variant with four mutations (M133L/V203A/N239Y/N268D) in the DNA-binding domain (2, 3) was used throughout the study. *Escherichia coli* BL21 cells transformed with plasmid encoding p53 were grown at 37 °C in 2× TY medium with 30 mg/mL kanamycin, and 0.1 mM Zn^{2+}. Isopropyl 1-thio-β-D-galactopyranoside (IPTG) was added to a final concentration of 1 mM at $O.D_{600} \sim 0.6$ to induce expression. After induction, cells were grown at 22 °C for 14 h, followed by harvesting and protein purification.

The cell pellets were resuspended in lysis buffer containing 50 mM NaP_i, pH 7.5, 150 mM NaCl, 5 mM DTT, and 15% glycerol and lysed using an Emulsiflex C5 high pressure homogenizer (Glen Creston). After centrifugation, the soluble fraction was subjected to several purification steps that include Ni-affinity column, TEV protease digestion, and Heparin HP column. The pooled fractions were purified further on a Superdex 200 26/60 preparative gel filtration column (Amersham Biosciences) in 25 mM NaP_i, pH 7.2, 150 mM NaCl, 5 mM DTT, and 10% glycerol. The purified p53 proteins were greater than 95% pure as judged by SDS-PAGE. Protein samples were flash-frozen and stored in liquid nitrogen for further use.

Isolation of p53·DNA tetramers. For isolation of p53 tetramers bound to DNA, solutions containing p53 at a concentration of 23 μM and the DNA probe at 30 μM were incubated for 30 min at room temperature, and then stored on ice. The reactions were performed in 25 mM sodium phosphate buffer, pH 7.2, 150 mM NaCl, 5 mM DTT, and 5% glycerol (vol/vol). The DNA probes were preannealed and contained the response element for gene GADD45 flanked by random nonspecific sequences (60-mer, 5′-CCTACAGAATCGCTCTACA**GAACATGTCTAAGCATGCT**GGGGACTGATGCTGGGGACTGG-3′, and complementary oligonucleotide; and 44-mer 5′-CCTACACTACA**GAACATGTCTAAGCATGCT**GGGGACTGGACTGG-3′, and complementary oligonucleotide). The samples were loaded in 15 mLl tubes with preformed glycerol (5%–30%) and glutaraldehyde (0%–0.15%) gradients, and centrifuged at 25,000 rpm for 18 h at 4 °C in rotor SW40Ti (Beckman). Gradient formation and fractionation was carried out using the Gradient Station and Piston Gradient Fractionator (Biocomp Instruments, Fredericton, Canada). This methodology is known as GraFix (4).

Electron microscopy and image processing. Selected fractions after gradient fractionation were adsorbed on carbon coated grids for 1 min, and then, a second carbon layer floating on a uranyl formate solution at 1% was fished. The resulting grids for EM contain a double carbon sandwich with the sample and the staining agent embedded between two carbon layers. EM samples were visualized in a JEM-2200FS (JEOL Europe, Croissy-sur-Seine, France) at 200 KV. Images were recorded on a 4 k × 4 k CCD camera at a magnification of ~67,000× resulting in a 2.1 Å final pixel size. Images were selected manually and the Contrast Transfer Function (CTF) corrected by flipping inverted frequencies. Reference-based projection matching was performed in EMAN (5) using a previously obtained EM model for p53 · DNA as a starting reference (6). Similar models were obtained using common-lines procedures in the same software package. Nonsupervised three-dimensional classification of the images for p53 · DNA complexes was performed by the maximum-likelihood based method (7) within the Xmipp package (8). Resolutions for the EM maps were calculated using cutoffs of 0.5 and 0.15 in the Fourier Shell Correlation (FSC) and the estimated values were in the range of 24–30 Å, values for the limit of resolution associated with negative staining and the grain size of the staining agent. Atomic coordinates for DBD · DNA complex [pdb code: 2ATA; (9)] and Tet domains [pdb code: 3SAK; (10)] were fitted as rigid bodies in Chimera (11), which was also used to produce figures.

Single molecule experiments. SM-FRET experiments were carried out on a home-built dual-channel confocal fluorescence microscope as described previously (12, 13). Gene encoding for the fragment p53 CTC (94–393) of human p53 was subcloned into Pet24a-HLTV plasmid. All the surface exposed cysteines (124, 182, 275, and 277) were mutated to alanine. Two cysteines were introduced at positions 292 and 372. Protein samples were labeled with Alexa fluor 546 and Alexa fluor 647 (Invitrogen, United Kingdom). After the reaction being quenched with 1 mM β-mercaptoethanol, the labeled protein was separated from the free dyes on a G-25 desalting column. The labeling efficiency was maintained low in order to avoid multiple labeling. 60-mer dsDNA, as used in EM studies, was used in single molecule experiments.

DNA constructs and production. Labeled DNA X1-20 (5′-Alexa488-GGACATGTCCGGACATGTCC) was purchased from Operon, whereas X2-20 (5′-fluorescein-GAAGATCTCCCAAGATCTTG) was purchased from Eurogentec, Belgium. Prior to use in experiments single-stranded sequences had to be annealed. X1-20 is palindromic and therefore self-annealing, whereas X2-20 was mixed in equimolar amounts with its reversed-complemented binding partner (CAAGATCTTGGGAGATCTTC). Oligonucleotides were annealed by heating to 95 °C for 5 min followed by cooling at 1 °C/min to room temperature in a PCR block (PTC-100, MJ Research Inc., USA). We constructed a plasmid containing approximately 1,000 base pairs (bp) of the p21 promoter with the p53 RE in the center. This plasmid was used to produce labeled DNA in sufficient quantities by performing several PCR reactions using FastStart PCR Master (Roche). As forward primers the labeled sequences X1 or X2 were used. Reverse primers were designed to guarantee appropriate sequence length. Samples were purified using the NucleoSpin Extract II columns (MachereyNagel) and purity was controlled by agarose gel electrophoresis. Concentration was measured using absorbance spectroscopy. Final sequences: X1-100 (5′-Alexa488-*GGACATGTCCGGACATGTCC*AGCTCTGGCATAGAAGAGGCTGGTGGCTATTTTGTCCTTGGGCTGCCTGTTTTCAGGTGAGGAAGGGGATGGTAGGAGACAGGAGACCCCACCCCCCCCACC, 122 bp), X2-100 (5′-fluorescein-*GAAGATCTCCCAAGATCTTG*AGCTCTGGCATAGAAGAGGCTGGTGGCTATTTTGTCCTTGGGCTGCCTGTTTTCAGGTGAGGAAGGGGATGGTAGGAGACAGGAGACCCCACCCCCCCCACC, 122 bp), X1-600 (5′-Alexa488-*GGACATGTCCGGACATGTCC*AGCTCTGGCATAGAAGAGGCTGGTGGCTATTTTGTCCTTGGGCTGCCTGTTTTCAGGTGAGGAAGGGGATGGTAGGAGACAGGAGACCTCTAAAGACCCCAGGTAAACCTTAGCCTGTTACTCTGAACAGGGTATGTGATCTGCCAGCA-

GATCCTTGCGACAGGGCTGGGATCTGATGCATGCGTG-CTTGTGTGAGTGTGTGCTGGGAGTCAGATTCTGTGTGT-GACTTTTAACAGCCTGCTCCCTTGCCTTCTTCAGGGCA-GAAGTCCTCCCTTAGAGTGTGTCTGGGAACACATT-CAAGTGCATGGTTGCAAACTTTTTTTTTAAAGCACT-GAATAGTACTAGACACTTAGTAGGTACTTAAGAAATATT-GAATGTCGTGGTGGTGGTGAGCAAGGGTGGGCGCGCC-GACCCAGCTTTCTTGTACAAAGTTGGCATTATAA-GAAAGCATTGCTTATCAATTTGTTGCAACGAACAGGT-CACTATCAGTCAAAATAAAATCATTATTTGCCATC-CAGCTGATATCCCCTATAGTGAGTCGTATTACATGGTCA-TAGCTGTTTCCTGCATATGAATTCGAAGCTTGAT, 609 bp).

Fluorescence anisotropy measurements. Fluorescence anisotropy was recorded on a FluoroMax-3 spectrometer (Horiba-Jobin Yvon) equipped with a titrator (Hamilton). Excitation and emission wavelength were 480 nm and 530 nm, respectively. Initial concentrations of labeled DNA solutions were between 2–5 nM. The concentration of the added protein solution varied between 250 nM and 10 μM depending on the affinity to the studied DNA sequence in order to obtain high quality titration curves. All experiments were performed at 20 °C in 5 mM DTT, 25 mM NaP_i (pH 7.2), 10% glycerol and 100, 150, or 225 mM NaCl, corresponding to low (122 mM), medium (172 mM) or high (247 mM) total ionic strength, respectively. Protein solution was titrated into a cuvette containing a stirred labeled DNA solution. Fluorescence intensities were measured after an equilibration time of 60 s. Data were analyzed using laboratory software as described (14). For low affinity interactions the expected final anisotropy values for protein DNA-complexes, which were known from the high-affinity interactions, were used for analysis.

1. Ang HC, Joerger AC, Mayer S, Fersht AR (2006) Effects of common cancer mutations on stability and DNA binding of full-length p53 compared with isolated core domains. *J Biol Chem* 281:21934–21941.
2. Joerger AC, Allen MD, Fersht AR (2004) Crystal structure of a superstable mutant of human p53 core domain. Insights into the mechanism of rescuing oncogenic mutations. *J Biol Chem* 279:1291–1296.
3. Nikolova PV, Henckel J, Lane DP, Fersht AR (1998) Semirational design of active tumor suppressor p53 DNA-binding domain with enhanced stability. *Proc Natl Acad Sci USA* 95:14675–14680.
4. Kastner B, et al. (2008) GraFix: sample preparation for single-particle electron cryomicroscopy. *Nat Methods* 5:53–55.
5. Ludtke SJ, Baldwin PR, Chiu W (1999) EMAN: semiautomated software for high-resolution single-particle reconstructions. *J Struct Biol* 128:82–97.
6. Tidow H, et al. (2007) Quaternary structures of tumor suppressor p53 and a specific p53 DNA complex. *Proc Natl Acad Sci USA* 104:12324–12329.
7. Scheres SH, et al. (2007) Disentangling conformational states of macromolecules in 3D-EM through likelihood optimization. *Nat Methods* 4:27–29.
8. Scheres SH, Nunez-Ramirez R, Sorzano CO, Carazo JM, Marabini R (2008) Image processing for electron microscopy single-particle analysis using XMIPP. *Nat Protoc* 3:977–990.
9. Kitayner M, et al. (2006) Structural basis of DNA recognition by p53 tetramers. *Mol Cell* 22:741–753.
10. Kuszewski J, Gronenborn AM, Clore GM (1999) Improving the packing and accuracy of NMR structure with a pseudopotential for the radius of gyration. *J Am Chem Soc* 121:2237–2338.
11. Pettersen EF, Goddard TD, Huang CC, Couch GS, Greenblatt DM, Meng EC, Ferrin TE (2004) UCSF Chimera—a visualization system for exploratory research and analysis. *J Comput Chem* 25:1605–1612.
12. Huang F, et al. (2009) Multiple conformations of full-length p53 detected with single-molecule fluorescence resonance energy transfer. *Proc Natl Acad Sci USA* 106:20758–20763.
13. Huang F, Ying L, Fersht AR (2009) Direct observation of barrier-limited folding of BBL by single-molecule fluorescence resonance energy transfer. *Proc Natl Acad Sci USA* 106:16239–16244.
14. Weinberg RL, Veprintsev DB, Fersht AR (2004) Cooperative binding of tetrameric p53 to DNA. *J Mol Biol* 341:1145–1159.

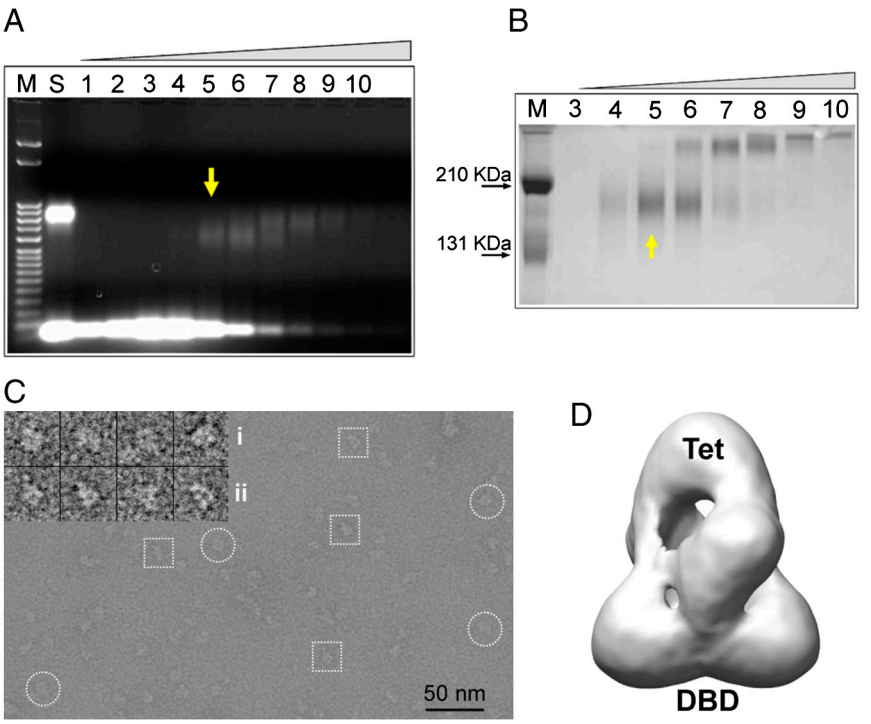

Fig. S1. Isolation and electron microscopy of p53 tetramers bound to DNA (*A*) and (*B*) After separation of p53 · DNA complexes through a glycerol/glutaraldehyde gradient, collected fractions were tested for the presence of complexes by EMSA (*A*) and SDS-PAGE (*B*). The yellow arrows in (*A*) and (*B*) indicate the fraction with p53 tetramers bound to DNA. (*C*) Field of electron micrograph for isolated p53 tetramers bound to DNA in negative stained technique. Some of the individual particles are enclosed by circles (globular shape) and squares (nonglobular ones). The inset at the top-left corner shows selected images with globular (*i*) or nonglobular (*ii*) shape. (*D*) Rendering of a three-dimensional EM map for a p53 · DNA complex obtained after image processing of EM data. Tet and DBD regions are labeled.

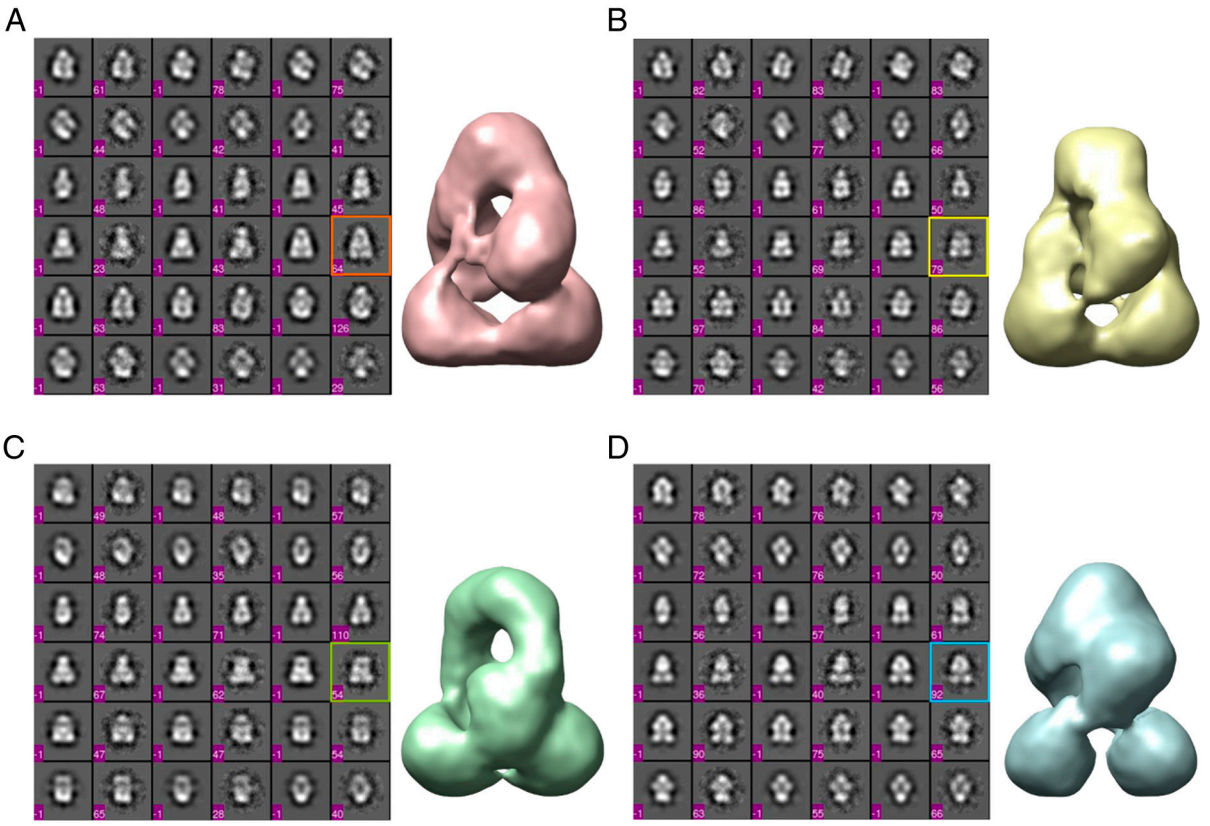

Fig. S2. Two-dimensional and three-dimensional data from ML3D classification for p53 tetramers on a 60-mer DNA Each shows a comparison between some of the projections of the three-dimensional maps and the corresponding class-averages for EM particles within the classes, together with rendering of the three-dimensional EM map for the class. The figures relate to classes I (*A*), II (*B*), III (*C*), and IV (*D*). In each, the two-dimensional projection that resembles the view of the three-dimensional map is highlighted, and the differences between the classes can be distinguished. Class-averages display the number of particles contributing to the average. The "−1" appearing in the projections for the three-dimensional map is meaningless.

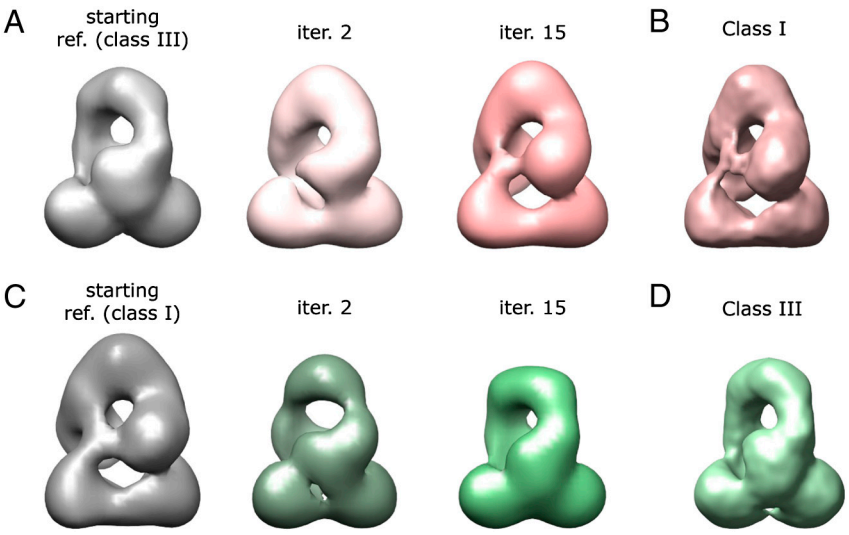

Fig. S3. Cross-refinement test for classes I and III. After ML3D classification of the total set of images for p53 tetramers on a 60 bp DNA probe, the consistency of the separation was tested by cross-refinement. Particles from each class were refined using three-dimensional EM maps from other classes. (*A*) Rendering of three-dimensional EM maps for the refinement of class I using map from class III as initial reference. The starting reference, the map after 2nd iteration, and the last map (iteration 15th) are rendered. It is clear that during the image processing, despite the use of class III as starting point, the map for class I emerges. (*B*) Display of the map for class I obtained during the ML3D classification. (*C*) Rendering of three-dimensional EM maps for the refinement of class III using map from class I as initial reference. The starting reference, the map after 2nd iteration, and the last map (iteration 15th) are rendered. Here also, the map for the corresponding class (class III) is obtained. (*D*) Display of the map for class III from the ML3D classification.

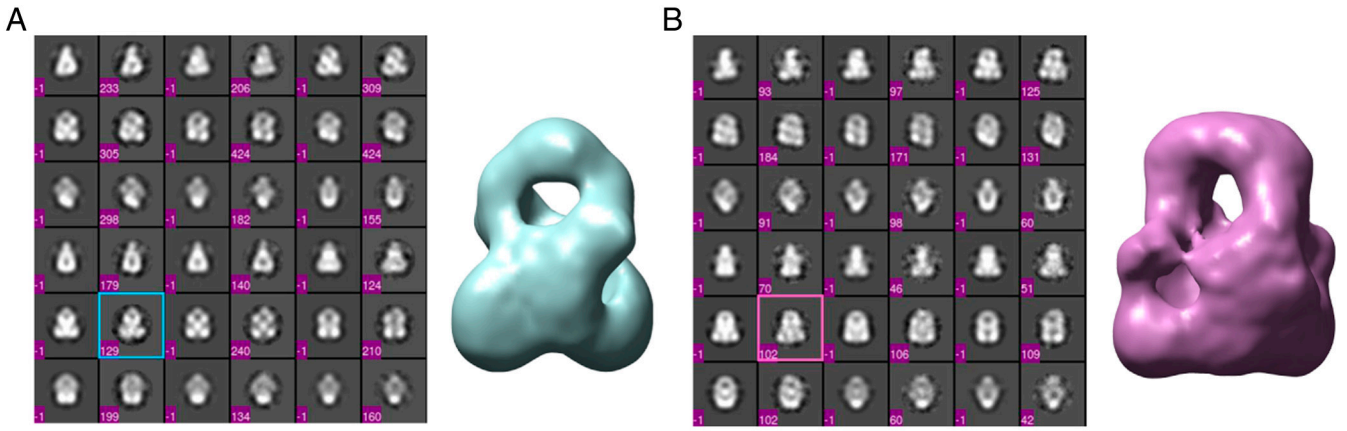

Fig. S4. Two-dimensional and three-dimensional data from ML3D classification for p53 tetramers on a 44-mer DNA. Each shows a comparison between some of the projections of the three-dimensional maps and the corresponding class-averages for EM particles within the classes, together with rendering of the three-dimensional EM map for the class. The figures relate to classes 2 (*A*), and 3 (*B*). In each, the two-dimensional projection that resembles the view of the three-dimensional map is highlighted. Class-averages display the number of particles contributing to the average. The "−1" appearing in the projections for the three-dimensional map is meaningless.

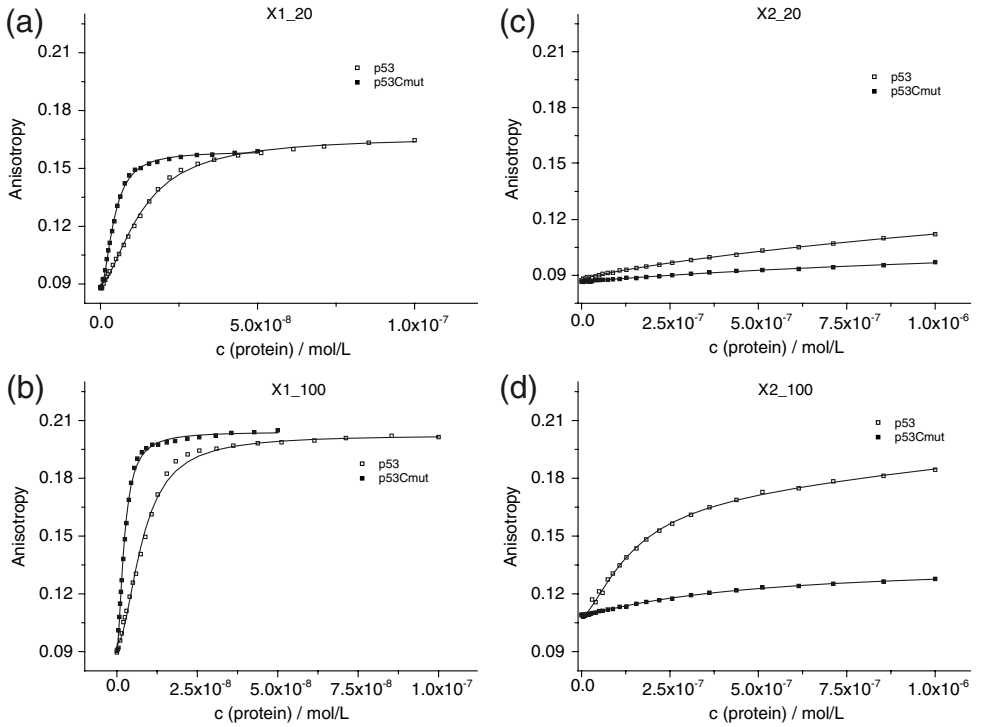

Fig. S5. Titration curves of fluorescence anisotropy experiments. *A*–*D*: Binding of X1-20 (*A*), X1-100 (*B*), X2-20 (*C*), and X2-100 (*D*) to p53 (hollow squares) and p53Cmut (filled squares).